Inclusive J/ψ and η_c production in Υ decay at $\mathcal{O}(\alpha_s^5)$ in nonrelativistic QCD factorization

Zhi-Guo He,[1,*] Bernd A. Kniehl[1,†] and Xiang-Peng Wang[1,2,‡]

[1]*II. Institut für Theoretische Physik, Universität Hamburg,*
Luruper Chaussee 149, 22761 Hamburg, Germany
[2]*High Energy Physics Division, Argonne National Laboratory, Argonne, Illinois 60439, USA*

We study J/ψ and η_c inclusive production in Υ decay within the framework of nonrelativistic-QCD (NRQCD) factorization. In the latter case, for which no experimental data exist so far, we also include the h_c feed-down contribution. We calculate the short-distance coefficients completely through $\mathcal{O}(\alpha_s^5)$. The NRQCD predictions for the branching fraction $\mathcal{B}(\Upsilon \to J/\psi + X)$ via direct production, evaluated with different sets of long-distance matrix elements (LDMEs), all agree with the experimental data in a reasonable range of renormalization scale. Using η_c and h_c LDMEs obtained from J/ψ and χ_c ones via heavy-quark spin symmetry, we find that the bulk of $\mathcal{B}(\Upsilon \to \eta_c + X)$ via prompt production arises from the $c\bar{c}(^3S_1^{[8]})$ Fock state. The experimental study of this decay process would, therefore, provide a particularly clean probe of the color octet mechanism of heavy-quarkonium production.

DOI: 10.1103/PhysRevD.101.074002

I. INTRODUCTION

Heavy-quarkonium production serves as an ideal laboratory to study the interplay of perturbative and non-perturbative phenomena of QCD thanks to the hierarchy of energy scales $m_Q v_Q^2 \ll m_Q v_Q \ll m_Q$ characterizing kinetic energy, momentum, and mass, where m_Q is the mass of the heavy quark Q and v_Q is its relative velocity in the rest frame of the heavy quarkonium. The effective quantum field theory of nonrelativistic QCD (NRQCD) [1] endowed with the factorization conjecture of Ref. [2] is the standard theoretical approach to study quarkonium production and decay. This conjecture states that the theoretical predictions can be separated into process-dependent short-distance coefficients (SDCs) calculated perturbatively as expansions in the strong-coupling constant α_s and supposedly universal long-distance matrix elements (LDMEs), scaling with definite powers of v_Q [3]. In this way, the theoretical calculations are organized as double expansion in α_s and v_Q.

During the past quarter of a century, the NRQCD factorization approach has been very successful in describing

*zhiguo.he@desy.de
†kniehl@desy.de
‡xiangpeng.wang@anl.gov

both heavy-quarkonium production and decay; see Refs. [4–6] for reviews. However, there are still open problems in charmonium production, in particular for the J/ψ meson. Prompt J/ψ production has been studied in various scenarios both experimentally and theoretically. Specifically, the SDCs are known at next-to-leading order (NLO) in α_s for the yield [7,8] and polarization [9] in e^+e^- annihilation, the yield in two-photon collisions [10–12], the yield [13] and polarization [14] in photoproduction, the yield [15,16] and polarization [17–20] in hadroproduction, etc. Different sets of LDMEs were obtained by fitting experimental data adopting different strategies. Unfortunately, none of them can explain all the experimental measurements, which challenges the universality of the NRQCD LDMEs. Moreover, it has been found [21] that all the LDME sets determined from J/ψ production data, upon conversion to η_c LDMEs via heavy-quark spin symmetry, result in NLO predictions that overshoot the η_c hadroproduction data, taken by the LHCb Collaboration at the CERN Large Hadron Collider (LHC) [22]. To shed more light on this notorious J/ψ puzzle, it is useful to consider yet further production modes. This provides an excellent motivation to study J/ψ and η_c inclusive production in Υ decays, which is the goal of this paper. This complements our recent study of χ_{cJ} inclusive production in Υ decays [23]. To facilitate the comparison with experimental data, we will focus here on direct J/ψ production, while we will consider prompt η_c production, by also including the feed-down from h_c mesons.

On the experimental side, the $\Upsilon \to J/\psi + X$ decay process was first observed by the CLEO Collaboration

at the Cornell Electron Storage Ring CESR about three decades ago [24]. Several independent measurements [25–27] followed. The latest one was carried out by the Belle Collaboration at the KEK B factory KEKB [28]. The present world average of the branching fraction for prompt production is [29]

$$\mathcal{B}_{\mathrm{prompt}}(\Upsilon \to J/\psi + X) = (5.4 \pm 0.4) \times 10^{-4}. \quad (1)$$

As for the $\Upsilon \to \eta_c + X$ decay, there is no experimental data yet. With the large amount of data to be accumulated by the Belle II Collaboration at the SuperKEKB accelerator, there might be a chance to study this process, and NRQCD predictions for its branching fraction will be needed.

On the theoretical side, the $\Upsilon \to J/\psi + X$ process was proposed as a rich gluon environment to study the color octet (CO) mechanism of NRQCD factorization in Refs. [30,31], where some of the CO channels, including $b\bar{b}(^3S_1^{[1]}) \to c\bar{c}(^3S_1^{[8]}) + gg$ at $\mathcal{O}(\alpha_s^4)$ and $b\bar{b}(^3S_1^{[1]}) \to c\bar{c}(^1S_0^{[8]}, ^3P_J^{[8]}) + g$ at $\mathcal{O}(\alpha_s^5)$, were taken into account. Later, the color singlet (CS) processes, including $b\bar{b}(^3S_1^{[1]}) \to c\bar{c}(^3S_1^{[1]}) + c\bar{c}g$ at $\mathcal{O}(\alpha_s^5)$, $b\bar{b}(^3S_1^{[1]}) \to c\bar{c}(^3S_1^{[1]}) + gg(gggg)$ at $\mathcal{O}(\alpha_s^6)$, and some interesting QED contribution were also calculated [32,33]. It was found that the CS contribution itself is about 3.8 times smaller than the experimental data, which suggests the potential need for a large CO contribution.

In the previous studies [30–33], only the leading-order (LO) $\mathcal{O}(\alpha_s^4)$ contribution and some part of the $\mathcal{O}(\alpha_s^5)$ channels were considered and pre-LHC LDME sets were used. In this work, we will obtain the complete SDC results through $\mathcal{O}(\alpha_s^5)$, both for J/ψ and η_c production, and perform a numerical analysis with up-to-date LDMEs sets. On top of direct production, prompt production also includes the feed-down from heavier charmonia, namely from χ_{cJ} and ψ' mesons in the J/ψ case and from h_c mesons in the η_c case. The direct J/ψ results obtained here readily carry over to ψ' feed-down, while the χ_{cJ} results may be found in Ref. [23]. The h_c feed-down results will also be derived here.

This paper is organized as follows. In Sec. II, we describe our analytical calculations. In Sec. III, we present and interpret our numerical results. Section IV contains our conclusions. In the Appendix, we list the contributing SDCs at $\mathcal{O}(\alpha_s^3)$.

II. ANALYTICAL CALCULATIONS

According to NRQCD factorization [2], the partial decay width of $\Upsilon \to H + X$ with $H = J/\psi, \eta_c, h_c$ is given by

$$\Gamma(\Upsilon \to H + X) = \sum_{m,n} \hat{\Gamma}_{mn} \langle \Upsilon | \mathcal{O}(m) | \Upsilon \rangle \langle \mathcal{O}^H(n) \rangle, \quad (2)$$

where $\hat{\Gamma}_{mn} = \hat{\Gamma}(b\bar{b}(m) \to c\bar{c}(n) + X)$ is the SDC and $\langle \Upsilon | \mathcal{O}(m) | \Upsilon \rangle$ and $\langle \mathcal{O}^H(n) \rangle$ are the LDMEs of Υ decay and H production, respectively.

For Υ, the CO contribution is so small [30] that we only include the CS case of $m = {}^3S_1^{[1]}$. In fact, by the velocity scaling rules [3], the leading CO LDMEs of Υ decay are parametrically suppressed by a factor of $v_b^4 \approx 1\%$ relative to the CS one, $\langle \Upsilon | \mathcal{O}(^3S_1^{[1]}) | \Upsilon \rangle$. In Ref. [34], the suppression factors for the S wave CO LDMEs of Υ decay were quantitatively determined in the framework of lattice NRQCD using two different schemes of implementing heavy-quark Green's functions, the hybrid and nrqcd schemes. The largest values were obtained in the hybrid scheme, namely, $\langle \Upsilon | \mathcal{O}(^1S_0^{[8]}) | \Upsilon \rangle / \langle \Upsilon | \mathcal{O}(^3S_1^{[1]}) | \Upsilon \rangle = 2.414(3) \times 10^{-3}$ and $\langle \Upsilon | \mathcal{O}(^3S_1^{[8]}) | \Upsilon \rangle / \langle \Upsilon | \mathcal{O}(^3S_1^{[1]}) | \Upsilon \rangle = 8.1(6) \times 10^{-5}$; see Table I in Ref. [34]. Similar analyses for the P wave LDME $\langle \Upsilon | \mathcal{O}(^3P_0^{[8]}) | \Upsilon \rangle$ are not yet available, but its suppression factor is expected to be in the same ballpark, of $\mathcal{O}(10^{-3})$ or below. On the other hand, SDCs involving CO $b\bar{b}$ Fock states m already start at $\mathcal{O}(\alpha_s^3)$. However, using $\alpha_s(m_b) \approx 0.26$, we have $\alpha_s^2 \approx 0.068 \gg 10^{-3}$, so that the contributions to Eq. (2) from the leading CO $b\bar{b}$ Fock states, $m = {}^1S_0^{[8]}, {}^3S_1^{[8]}, {}^3P_J^{[8]}$, are expected to be safely negligible against the $\mathcal{O}(\alpha_s^5)$ contributions with $m = {}^3S_1^{[1]}$, which we still include here. For future use, we list the $\mathcal{O}(\alpha_s^3)$ SDCs $\hat{\Gamma}_{mn}$ for all the decay processes considered here and in Ref. [23], $\Upsilon \to H + X$ with $H = J/\psi, \eta_c, \chi_{cJ}, h_c$, in the Appendix.

On the other hand, for H, we include the CO contributions of LO in v_c^2 besides the CS contributions, i.e., we have $n = {}^3S_1^{[1,8]}, {}^1S_0^{[8]}, {}^3P_J^{[8]}$ for J/ψ, $n = {}^1S_0^{[1,8]}, {}^3S_1^{[8]}, {}^1P_1^{[8]}$ for η_c, and $n = {}^1P_1^{[1]}, {}^1S_0^{[8]}$ for h_c.

In our computation, we generate all the Feynman amplitudes using the FEYNARTS package [35]. The Dirac and color operations are performed with the help of the FEYNCALC [36] and FORM [37] packages. We use the Mathematica package $Apart [38] to decompose linearly dependent propagators in the loop integrals to irreducible ones, which we further reduce to master scalar integrals using the FIRE package [39]. We then evaluate the master integrals numerically using the C++ package QCDLOOP [40]. Finally, we perform the phase space integrations numerically using the CUBA [41] library.

The $\mathcal{O}(\alpha_s^4)$ LO contribution only includes the $b\bar{b}(^3S_1^{[1]}) \to c\bar{c}(^3S_1^{[8]}) + gg$ subprocess. Its NLO QCD corrections, of $\mathcal{O}(\alpha_s^5)$, were calculated in our previous work [23], where details may be found. Here, we only present numerical results. At $\mathcal{O}(\alpha_s^5)$, also a number of new partonic production channels open up. We derive here the SDCs of all of them. In the cases where results already exist in the literature, we compare and find agreement. For the sake of a systematical discussion, we divide the contributing partonic subprocesses into three groups according to the parton content of the system X in the final state: (a) $X = g$, (b) $X = ggg$, and (c) $X = c\bar{c}g$. Representative Feynman diagrams for each group are shown in Fig. 1.
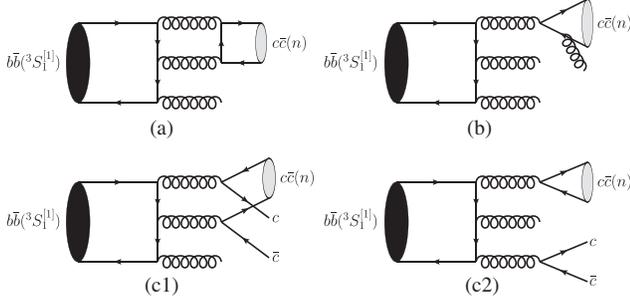
FIG. 1. Representative Feynman diagrams for subprocesses $b\bar{b}(^3S_1^{[1]}) \to c\bar{c}(n) + X$, with (a) $X = g$, (b) $X = ggg$, and (c) $X = c\bar{c}g$. The possible $c\bar{c}$ Fock states include $n = {}^1S_0^{[8]}, {}^3P_J^{[8]}$ in group (a), $n = {}^1S_0^{[1,8]}, {}^1P_1^{[8]}, {}^3P_J^{[8]}$ in group (b), $n = {}^1S_0^{[1,8]}, {}^3S_1^{[1,8]}, {}^1P_1^{[1,8]}, {}^3P_J^{[8]}$ in subgroup (c1), and $n = {}^3S_1^{[8]}$ in subgroup (c2).

In group (a), the only possible $c\bar{c}$ Fock states are $n = {}^1S_0^{[8]}, {}^3P_J^{[8]}$, and there are 6 Feynman diagrams, a typical one of which is shown in panel (a) of Fig. 1. The SDCs of these partonic subprocesses were first calculated in Ref. [31]. We evaluate the one-loop amplitude of $b\bar{b}(^3S_1^{[1]}) \to c\bar{c}(^1S_0^{[8]}) + g$ applying the helicity projector approach [42] and the one of $b\bar{b}(^3S_1^{[1]}) \to c\bar{c}(^3P_J^{[8]}) + g$ as the virtual corrections in Ref. [23]. We find agreement with Ref. [31].

In group (b), the possible $c\bar{c}$ Fock states are $n = {}^1S_0^{[1,8]}, {}^1P_1^{[8]}, {}^3P_J^{[8]}$, and there are 36 Feynman diagrams, a representative one of which is displayed in panel (b) of Fig. 1. None of these partonic subprocesses have been studied before. Except for $n = {}^3P_J^{[8]}$, all the SDCs are infrared finite and straightforwardly calculated. The infrared divergence in the SDC of $b\bar{b}(^3S_1^{[1]}) \to c\bar{c}(^3P_J^{[8]}) + ggg$ can be extracted by means of the phase space slicing method [43], as explained in detail for the CS case of $^3P_J^{[1]}$ in Ref. [23]. In NRQCD factorization, this infrared divergence is absorbed into the NLO corrections to the CO LDME $\langle \mathcal{O}^{J/\psi}(^3S_1^{[8]}) \rangle$ [2,44],

$$\langle \mathcal{O}^{J/\psi}(^3S_1^{[8]}) \rangle_{\text{Born}}$$
$$= \langle \mathcal{O}^{J/\psi}(^3S_1^{[8]}) \rangle_{\text{ren}}$$
$$+ \frac{2\alpha_s}{3\pi m_c^2} \left(\frac{4\pi\mu^2}{\mu_\Lambda^2} e^{-\gamma_E} \right)^\epsilon \frac{1}{\epsilon_{\text{IR}}} \sum_J \left[\frac{C_F}{C_A} \langle \mathcal{O}^{J/\psi}(^3P_J^{[1]}) \rangle_{\text{Born}} \right.$$
$$\left. + \left(\frac{C_A}{2} - \frac{2}{C_A} \right) \langle \mathcal{O}^{J/\psi}(^3P_J^{[8]}) \rangle_{\text{Born}} \right], \quad (3)$$

where $\langle \mathcal{O}^{J/\psi}(^3S_1^{[8]}) \rangle_{\text{ren}}$ is the renormalized LDME, μ and μ_Λ are the QCD and NRQCD factorization scales, respectively, $\epsilon = 2 - d/2$ in d space-time dimensions, and $C_F = 4/3$ and $C_A = 3$ are color factors. We verified numerically that
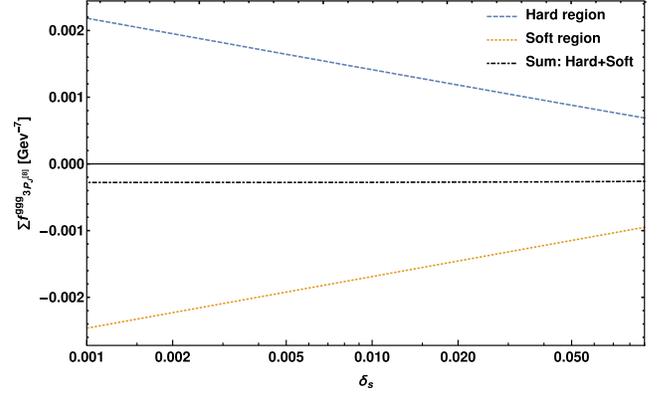
FIG. 2. Numerical dependence on the phase space slicing parameter δ_s of the soft (dotted line) and hard (dashed line) parts of the SDC of $b\bar{b}(^3S_1^1) \to c\bar{c}(^3P_J^{[8]}) + ggg$ as well as their superposition (dot-dashed line) upon subtraction of the infrared divergence at NRQCD factorization scale $\mu_\Lambda = m_c$.

the finite piece left over after removing the infrared divergence does not depend on the slicing parameter δ_s, which is illustrated in Fig. 2.

In group (c), all the relevant $c\bar{c}$ Fock states $n = {}^1S_0^{[1,8]}, {}^3S_1^{[1,8]}, {}^1P_1^{[1,8]}, {}^3P_J^{[8]}$ appear. There are generally 6 Feynman diagrams similar to the one shown in panel (c1) of Fig. 1, with the exception of $n = {}^3S_1^{[8]}$ for which there are 6 additional ones of fragmentation type as in panel (c2). The SDC of $b\bar{b}(^3S_1^{[1]}) \to c\bar{c}(^3S_1^{[1]}) + c\bar{c}g$ was first considered in Ref. [45], and the correct result was first presented in Ref. [32]. All the other partonic subprocesses are studied here for the first time. Their SDCs are all infrared finite and can be calculated straightforwardly.

To be able to investigate the relative weight of each partonic subprocess, we decompose $\hat{\Gamma}_{{}^3S_1^{[1]},n}$ for each n according to the possible final-state systems X,

$$\hat{\Gamma}_{{}^3S_1^{[1]},n} = \sum_X \hat{\Gamma}_n^X, \quad (4)$$

where $X = gg, ggg, c\bar{c}g$ for $n = {}^3S_1^{[8]}$, $X = g, ggg, c\bar{c}g$ for $n = {}^1S_0^{[8]}, {}^3P_J^{[8]}$, $X = ggg, c\bar{c}g$ for $n = {}^1S_0^{[1]}, {}^1P_1^{[8]}$, and $X = c\bar{c}g$ for $n = {}^3S_1^{[1]}, {}^1P_1^{[1]}$. Furthermore, we factor out the strong-coupling constant $\alpha_s(\mu)$ and render the coefficients dimensionless by writing

$$\hat{\Gamma}_{{}^3S_1^{[8]}}^{gg} = [f_{{}^3S_1^{[8]}}^{gg,\text{LO}} + f_{{}^3S_1^{[8]}}^{gg,\text{corr}}(\mu)\alpha_s(\mu)]\alpha_s^4(\mu) \text{ GeV}^{-5},$$
$$\hat{\Gamma}_n^X = f_n^X \alpha_s^5(\mu) \text{ GeV}^{-k}, \quad (5)$$

where $k = 5$ for $n = {}^3S_1^{[8]}$ with $X = c\bar{c}g$ and $n = {}^1S_0^{[1,8]}, {}^3S_1^{[1]}$, and $k = 7$ for $n = {}^1P_1^{[1,8]}, {}^3P_J^{[8]}$.

TABLE I.   Numerical results for the dimensionless coefficients f_n^X in Eq. (5) besides $f_{3S_1^{[8]}}^{gg,\text{corr}} = (4.85 + 13.62 \times \ln\frac{\mu}{m_b}) \times 10^{-4}$.

$f^{ggg}_{1S_0^{[1]}}$	$f^{c\bar{c}g}_{1S_0^{[1]}}$	$f^{c\bar{c}g}_{3S_1^{[1]}}$	$f^{c\bar{c}g}_{1P_1^{[1]}}$	$f^{g}_{1S_0^{[8]}}$	$f^{ggg}_{1S_0^{[8]}}$	$f^{c\bar{c}g}_{1S_0^{[8]}}$	$f^{gg,\text{LO}}_{3S_1^{[8]}}$	$f^{c\bar{c}g}_{3S_1^{[8]}}$	$f^{ggg}_{1P_1^{[8]}}$	$f^{c\bar{c}g}_{1P_1^{[8]}}$	$f^{g}_{3P_J^{[8]}}$	$f^{ggg}_{3P_J^{[8]}}$	$f^{c\bar{c}g}_{3P_J^{[8]}}$
1.89×10^{-6}	1.07×10^{-6}	1.32×10^{-6}	1.5×10^{-7}	1.15×10^{-4}	1.50×10^{-5}	2.14×10^{-6}	2.38×10^{-4}	1.23×10^{-5}	6.4×10^{-7}	3.0×10^{-7}	1.97×10^{-4}	-2.78×10^{-4}	1.3×10^{-6}

III. NUMERICAL RESULTS

In our numerical analysis, we evaluate $\alpha_s(\mu)$ with $n_f = 3$ massless quark flavors and $\Lambda_{\text{QCD}} = 249(389)$ MeV at LO (NLO), set $m_c = 1.5$ GeV, $m_b = 4.75$ GeV, and choose $\mu_\Lambda = m_c$. The resulting values of f_n^X are presented in Table I. The only instance where the LO formula for $\alpha_s(\mu)$ is used is in the LO evaluation of $\hat{\Gamma}^{gg}_{3S_1^{[8]}}$ in Eq. (5) with $f_{3S_1^{[8]}}^{gg,\text{corr}}(\mu)$ put to zero.

Given the large powers of $\alpha_s(\mu)$ appearing in Eq. (5), we are faced with considerable μ dependencies, so that scale optimization appears appropriate. As in Ref. [23], we adopt the principle of fastest apparent convergence (FAC) [46] to determine the default value of μ, by requiring that the LO and NLO evaluations of $\hat{\Gamma}^{gg}_{3S_1^{[8]}}$ as described above coincide. This yields $\mu_{\text{FAC}} = 6.2$ GeV. It would then be natural to explore the μ dependence in the range $\mu_{\text{FAC}}/2 < \mu < 2\mu_{\text{FAC}}$. However, the NLO result for $\mathcal{B}(\Upsilon \to \chi_{c0} + X)$ is known to be negative for $\mu < 3.7$ GeV [23]. We thus consider the reduced μ range 3.7 GeV $< \mu < 2\mu_{\text{FAC}}$ in the following.

When the $b\bar{b}$ pair is in a CS Fock state, it couples to at least three gluons in the decays $\Upsilon \to H + X$ with $H = J/\psi, \eta_c, h_c$, as may be seen in Fig. 1. Therefore, the large theoretical uncertainty due to the freedom in the choices of α_s and m_b can be greatly reduced by normalizing $\Gamma(\Upsilon \to H + X)$ with respect to $\Gamma(\Upsilon \to ggg)$ [23,32,33]. We thus write the branching fractions of interest as

$$\mathcal{B}(\Upsilon \to H + X) = \frac{\Gamma(\Upsilon \to H + X)}{\Gamma(\Upsilon \to ggg)} \mathcal{B}(\Upsilon \to ggg), \quad (6)$$

where $\mathcal{B}(\Upsilon \to ggg) = 81.7\%$ [29]. Through $\mathcal{O}(\alpha_s^4)$, we have [47]

$$\Gamma(\Upsilon \to ggg)$$
$$= \frac{20\alpha_s^3(\mu)}{243m_b^2}(\pi^2 - 9)\langle\Upsilon|\mathcal{O}(^3S_1^{[1]})|\Upsilon\rangle$$
$$\times \left\{ 1 + \frac{\alpha_s(\mu)}{\pi}\left[-19.4 + \frac{3\beta_0}{2}\left(1.161 + \ln\frac{\mu}{m_b} \right) \right] \right\}, \quad (7)$$

where $\beta_0 = 11 - 2n_f/3$ with $n_f = 4$. As an additional benefit, the theoretical predictions do not depend on the CS LDME $\langle\Upsilon|\mathcal{O}(^3S_1^{[1]})|\Upsilon\rangle$ anymore.

A. $\Upsilon \to J/\psi + X$

We first discuss $\Upsilon \to J/\psi + X$ via direct production. From Table I, we observe that all $c\bar{c}$ Fock states $^3S_1^{[1]}$, $^3S_1^{[8]}$, $^1S_0^{[8]}$, $^3P_J^{[8]}$ contribute significantly as long as the values of the corresponding LDMEs are not too small. Incidentally, there is a strong cancellation between the $c\bar{c}(^3P_J^{[8]}) + g$ and $c\bar{c}(^3P_J^{[8]}) + ggg$ channels, the latter one being studied here for the first time. Several J/ψ LDME sets have been determined, both at LO and NLO, by fitting to different sets of J/ψ yield and polarization data. There are significant differences between them, which reflects the potential challenge to NRQCD factorization mentioned above. We select here the ones most frequently used in the recent literature [12,19,48–50] and summarize their values in Table II. Besides the contributions through $\mathcal{O}(\alpha_s^5)$ discussed above, we will also include some other nonnegligible contributions previously studied, namely the pure CS contributions at $\mathcal{O}(\alpha_s^2\alpha^2)$ [32] and $\mathcal{O}(\alpha_s^6)$ [33]. From Ref. [29], we extract the result for direct J/ψ production,

$$\mathcal{B}_{\text{direct}}(\Upsilon \to J/\psi + X) = (3.46 \pm 0.67) \times 10^{-4}, \quad (8)$$

TABLE II. J/ψ LDME sets from Refs. [12,18,19,48–50]. Set 3 of Ref. [18] only gave an upper bound on $\langle\mathcal{O}^{J/\psi}(^1S_0^{[8]})\rangle$ and is replaced here by its update in Ref. [48].

J/ψ LDME set	Butenschön et al. [12,49]	Gong et al. [19]	Bodwin et al. [50]	Chao et al. Default set [18]	Chao et al. Set 2 [18]	Chao et al. Set 3 [48]
$\langle\mathcal{O}^{J/\psi}(^3S_1^{[1]})\rangle/\text{GeV}^3$	1.32	1.16	1.32	1.16	1.16	1.16
$\langle\mathcal{O}^{J/\psi}(^1S_0^{[8]})\rangle/\text{GeV}^3$	0.0304 ± 0.0035	0.097 ± 0.009	0.110 ± 0.014	0.089 ± 0.0098	0	0.0146 ± 0.0020
$\langle\mathcal{O}^{J/\psi}(^3S_1^{[8]})\rangle/\text{GeV}^3$	0.00168 ± 0.00046	-0.0046 ± 0.0013	-0.00713 ± 0.00364	0.0030 ± 0.0012	0.014	0.00903 ± 0.00275
$\langle\mathcal{O}^{J/\psi}(^3P_0^{[8]})\rangle/\text{GeV}^5$	-0.00908 ± 0.00161	-0.0214 ± 0.0056	-0.00702 ± 0.00340	0.0126 ± 0.0047	0.054	0.0343 ± 0.0110

TABLE III. Fitted μ_{fit} values for the J/ψ LDME sets in Table II.

J/ψ LDME set	μ_{fit} (GeV)
Butenschön et al. [12,49]	3.8
Gong et al. [19]	3.9
Bodwin et al. [50]	3.7
Chao et al. (Default) [18]	4.6
Chao et al. (Set 2) [18]	5.1
Chao et al. (Set 3) [48]	4.2

by subtracting the contributions due to the feed-down from the χ_{cJ} and ψ' mesons. In Fig. 3, we confront it with our NRQCD predictions evaluated with the J/ψ LDME sets listed in Table II as functions of μ. We observe from Fig. 3 that, although the various predictions appreciably differ in normalization and line shape, each of them can describe the experimental data in a plausible region of μ. For each of the considered J/ψ LDME sets, we determine the value of μ, μ_{fit}, where the respective theoretical prediction coincides with the central value of the experimental result and list it in Table III. We observe from Table III that these μ_{fit} values all fall into the preferred range 3.7 GeV $< \mu < 2\mu_{\text{FAC}}$ and thus conclude that NRQCD factorization is compatible with experiment here. However, we caution the reader that the J/ψ LDME sets of Refs. [12,19,49,50] yield μ_{fit} values that are rather close to the border at 3.7 GeV, below which the NLO prediction for $\mathcal{B}(\Upsilon \to \chi_{c0} + X)$ is negative [23].

B. $\Upsilon \to \chi_{cJ} + X$

At this point, we briefly address $\Upsilon \to J/\psi + X$ via the feed-down from χ_{cJ} mesons, i.e., via $\Upsilon \to \chi_{cJ} + X$ followed by $\chi_{cJ} \to J/\psi + \gamma$. In Ref. [23], we determined the χ_{c0} CO LDME to be $\langle \mathcal{O}^{\chi_{c0}}(^3S_1^{[8]}) \rangle = (4.04 \pm 0.47^{+0.67}_{-0.34}) \times 10^{-3}$ GeV^3 by adopting the χ_{c0} CS LDME $\langle \mathcal{O}^{\chi_{c0}}(^3P_0^{[1]}) \rangle = 0.107$ GeV^5 from the analysis of Ref. [51] with the Buchmüller-Type potential [52] and so fitting experimental data of $\mathcal{B}(\Upsilon \to \chi_{c1} + X)$ and $\mathcal{B}(\Upsilon \to \chi_{c2} + X)$. Using these χ_{c0}

LDMEs, we find that about 20% of $\mathcal{B}(\Upsilon \to J/\psi + X)$ via prompt production is due to the feed-down from χ_{cJ} mesons.

C. $\Upsilon \to \eta_c + X$

We now discuss $\Upsilon \to \eta_c + X$ via prompt production. The LDMEs of η_c and h_c production are related to those of J/ψ and χ_c production via heavy-quark spin symmetry (HQSS) at LO in v_c^2 as

$$\langle \mathcal{O}^{\eta_c}(^1S_0^{[1,8]}) \rangle = \frac{1}{3} \langle \mathcal{O}^{J/\psi}(^3S_1^{[1,8]}) \rangle,$$

$$\langle \mathcal{O}^{\eta_c}(^3S_1^{[8]}) \rangle = \langle \mathcal{O}^{J/\psi}(^1S_0^{[8]}) \rangle,$$

$$\langle \mathcal{O}^{\eta_c}(^1P_1^{[8]}) \rangle = 3 \langle \mathcal{O}^{J/\psi}(^3P_0^{[8]}) \rangle,$$

$$\langle \mathcal{O}^{h_c}(^1P_1^{[1]}) \rangle = 3 \langle \mathcal{O}^{\chi_{c0}}(^3P_0^{[1]}) \rangle,$$

$$\langle \mathcal{O}^{h_c}(^1S_0^{[8]}) \rangle = 3 \langle \mathcal{O}^{\chi_{c0}}(^3S_1^{[8]}) \rangle. \tag{9}$$

We now evaluate $\mathcal{B}(\Upsilon \to \eta_c + X)$ via direct production using the SDCs in Table I together with the η_c LDMEs converted from Table II via Eq. (9) and present the results as functions of μ in Fig. 4. The corresponding results at $\mu = \mu_{\text{FAC}}$ are listed in Table IV. For comparison, we also present there the results at $\mu = \mu_{\text{fit}}$ for the individual μ_{fit} values in Table III. We observe from Fig. 4 and the entries in Table IV for the common scale choice $\mu = \mu_{\text{FAC}}$ that the results for the J/ψ LDME sets from Refs. [19,50] and the default one from Ref. [18] are very similar, quite in contrast to the findings in Fig. 3 and Table III. This may be traced to the approximate agreement of the respective values of $\langle \mathcal{O}^{J/\psi}(^1S_0^{[8]}) \rangle$ in Table II by noticing that, similarly to the case of η_c hadroproduction [21], the bulk of the NRQCD prediction is made up by the $^3S_1^{[8]}$ channel alone. The latter observation can be easily made from Fig. 5, where the various NRQCD predictions for $\mathcal{B}_{\text{direct}}(\Upsilon \to \eta_c + X)$ in Fig. 4 are decomposed into the $^3S_1^{[8]}$ contributions and the

FIG. 3. μ dependencies of the NRQCD predictions for $\mathcal{B}_{\text{direct}}(\Upsilon \to J/\psi + X)$ based on the J/ψ LDME sets in Table II compared with the experimental result in Eq. (8).
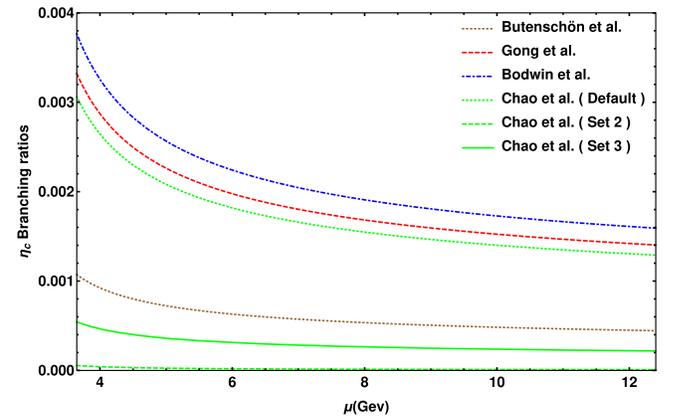
FIG. 4. μ dependencies of the NRQCD predictions for $\mathcal{B}_{\text{direct}}(\Upsilon \to \eta_c + X)$ based on the η_c LDME sets obtained from Table II via Eq. (9).
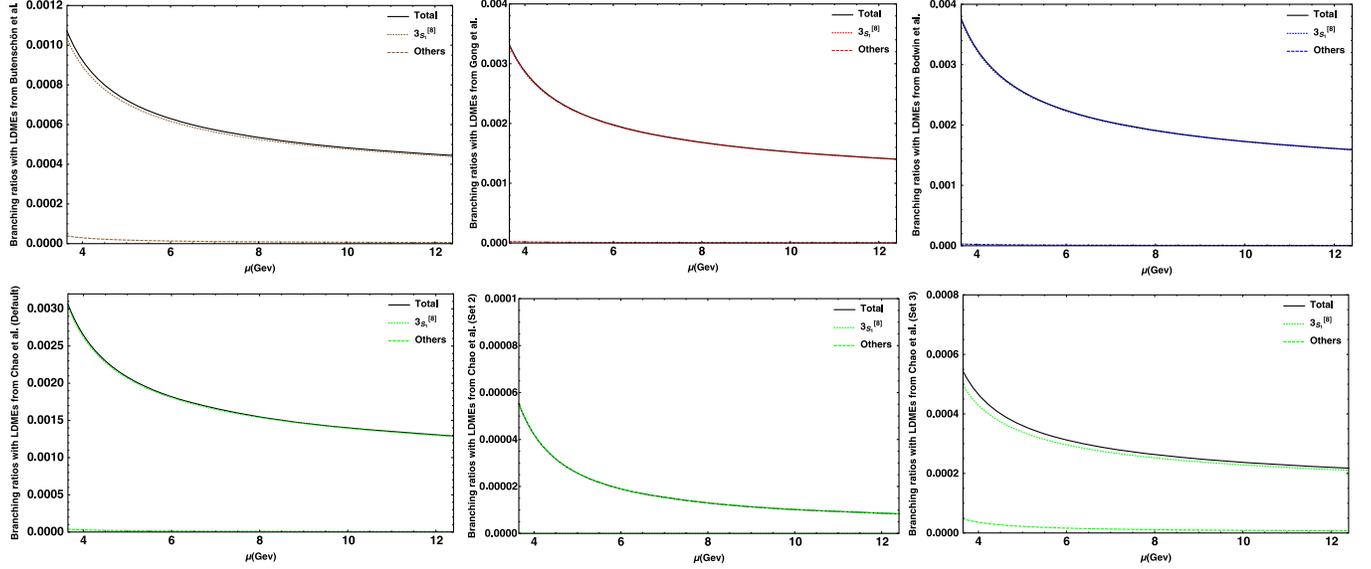
FIG. 5.   The results in Fig. [4] (solid lines) are decomposed into their $^3S_1^{[8]}$ contributions (dotted lines) and the rest (dashed lines).

rest. In the special case of Set 2 of the J/ψ LDMEs from Ref. [18], where $\langle \mathcal{O}^{J/\psi}(^1S_0^{[8]}) \rangle = 0$, the $^3S_1^{[8]}$ channel of η_c production is quenched leading to a particularly small NRQCD prediction for $\mathcal{B}_{\text{direct}}(\Upsilon \to \eta_c + X)$.

In the case of η_c inclusive hadroproduction, it was found at NLO that the CS channel alone exhausts the cross section measured by the LHCb Collaboration [22], while the complete NRQCD predictions overshoot it by a few times to an order of magnitude depending on the LDME set chosen [21]. It is, therefore, interesting to examine the importance of CO processes for $\Upsilon \to \eta_c + X$. We find that the CS contribution to $\mathcal{B}_{\text{direct}}(\Upsilon \to \eta_c + X)$ ranges from 3.2×10^{-5} to 0.5×10^{-5} for 3.7 GeV $< \mu < 2\mu_{\text{FAC}}$ and takes the value 1.1×10^{-5} for $\mu = \mu_{\text{FAC}}$, which is about 1.6 times smaller than the smallest NRQCD prediction for

TABLE IV.   Values of $\mathcal{B}_{\text{direct}}(\Upsilon \to \eta_c + X)$ from Fig. [4] at $\mu = \mu_{\text{FAC}}$ and $\mu = \mu_{\text{fit}}$.

J/ψ LDME set	$\mu = \mu_{\text{FAC}}$	$\mu = \mu_{\text{fit}}$
Butenschön *et al.* [12,49]	6.2×10^{-4}	1.0×10^{-3}
Gong *et al.* [19]	1.9×10^{-3}	3.0×10^{-3}
Bodwin *et al.* [50]	2.2×10^{-3}	3.7×10^{-3}
Chao *et al.* (Default) [18]	1.8×10^{-3}	2.3×10^{-3}
Chao *et al.* (Set 2) [18]	1.8×10^{-5}	2.5×10^{-5}
Chao *et al.* (Set 3) [48]	3.1×10^{-4}	4.3×10^{-4}

$\mu = \mu_{\text{FAC}}$ in Table IV, for Set 2 of the J/ψ LDMEs from Ref. [18], and more than one or even two orders of magnitude smaller than NRQCD predictions for the other J/ψ LDMEs sets. In other words, $\Upsilon \to \eta_c + X$ is predicted to proceed even more dominantly through CO processes than η_c inclusive hadroproduction. We thus conclude that the study of $\Upsilon \to \eta_c + X$ is expected to provide a crucial test of the CO mechanism of NRQCD factorization and to place valuable constraints on the CO LDMEs of J/ψ production, in particular on $\langle \mathcal{O}^{J/\psi}(^1S_0^{[8]}) \rangle$, assuming that HQSS is preserved.

Finally, we caution the reader that, in the case of $\mathcal{B}_{\text{direct}}(\Upsilon \to \eta_c + X)$, the CO contributions from the initial state may be somewhat less suppressed than expected from the velocity scaling rules [3]. In fact, comparing the entry for the J/ψ LDMEs of Refs. [12,49] and $\mu = \mu_{\text{FAC}}$ (μ_{fit}) in Table IV with the respective entry for the hybrid scheme in Table V, we observe that the contribution due to the S wave CO $b\bar{b}$ Fock states reaches about 26% (16%) of our default result.

D. $\Upsilon \to h_c + X$

Finally, we turn to $\Upsilon \to \eta_c + X$ via the feed-down from h_c mesons, i.e., via $\Upsilon \to h_c + X$ followed by $h_c \to \eta_c + \gamma$. Converting the LDMEs for χ_{c0} production quoted above to those of h_c production via the appropriate HQSS relations

TABLE V. $\mathcal{O}(\alpha_s^3)$ contributions to $\mathcal{B}_{\text{direct}}(\Upsilon \to H + X)$ for $H = J/\psi, \eta_c, \chi_{cJ}, h_c$ due to the S wave CO $b\bar{b}$ Fock states.

scheme	J/ψ	η_c	χ_{c0}	χ_{c1}	χ_{c2}	h_c
hybrid	8.3×10^{-6}	1.6×10^{-4}	2.0×10^{-5}	2.2×10^{-5}	2.1×10^{-5}	2.0×10^{-7}
nrqcd	5.0×10^{-7}	9.0×10^{-6}	8.3×10^{-7}	1.7×10^{-6}	1.2×10^{-6}	1.7×10^{-7}
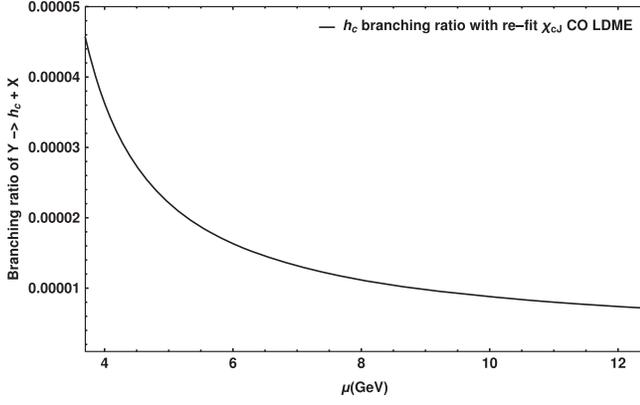
FIG. 6. μ dependence of NRQCD prediction for $\mathcal{B}(\Upsilon \to h_c + X)$ based on the h_c LDME set obtained from Ref. [23] via Eq. (9).

in Eq. (9), we obtain $\langle \mathcal{O}^{h_c}(^1P_1^{[1]}) \rangle = 0.321 \text{ GeV}^5$ and $\langle \mathcal{O}^{h_c}(^1S_0^{[8]}) \rangle = (1.21 \pm 0.15^{+0.20}_{-0.10}) \times 10^{-2} \text{ GeV}^3$. The resulting NRQCD prediction for $\mathcal{B}(\Upsilon \to h_c + X)$ is presented as a function of μ in Fig. 6. At $\mu = \mu_{\text{FAC}}$, we have $\mathcal{B}(\Upsilon \to h_c + X) = 1.6 \times 10^{-5}$. Taking into account the branching fraction $\mathcal{B}(h_c \to \eta_c + X) = 51\%$ [29], the feed-down contribution is found to be $\mathcal{B}_{h_c \text{feed down}}(\Upsilon \to \eta_c + X) = 8.0 \times 10^{-6}$ at $\mu = \mu_{\text{FAC}}$.

IV. CONCLUSIONS

In summary, we studied J/ψ and η_c inclusive production via Υ decay in the NRQCD factorization approach, including also the feed-down from h_c mesons in the latter case. We calculated the SDCs completely through $\mathcal{O}(\alpha_s^5)$ keeping the $b\bar{b}$ pair in the $^3S_1^{[1]}$ CS Fock state, but including all the relevant $c\bar{c}$ Fock states, both the $^1S_0^{[1]}$, $^3S_1^{[1]}$, and $^1P_1^{[1]}$ CS ones and the $^1S_0^{[8]}$, $^3S_1^{[8]}$, $^1P_1^{[8]}$, and $^3P_J^{[8]}$ CO ones, and allowing for all possible combinations of gluons or open $c\bar{c}$ pairs to accompany the charmonia.

As for $\Upsilon \to J/\psi + X$ via direct production, we found that the NLO sets of J/ψ LDMEs recently determined from fits to experimental data of inclusive production at various types of colliders or just hadron colliders all lead to useful interpretations of the measured branching fraction, in the sense that the renormalization scale μ_{fit} which yields

agreement with the central value is in the ballpark of the optimal scale $\mu_{\text{FAC}} = 6.2 \text{ GeV}$ of the FAC principle.

In want of direct determinations, we relied on η_c and h_c LDMEs obtained from J/ψ and χ_{cJ} ones via HQSS relations. As for $\Upsilon \to \eta_c + X$ via prompt production, we thus predicted the branching fraction to range between 2.6×10^{-5} and 2.2×10^{-3} at $\mu = \mu_{\text{FAC}}$, with a strong dependence on the choice of LDMEs, in particular on the value of $\langle \mathcal{O}^{\eta_c}(^3S_1^{[8]}) \rangle$. On the contrary, the CS contribution to $\mathcal{B}_{\text{prompt}}(\Upsilon \to \eta_c + X)$ amounts to just about 1.1×10^{-5} at $\mu = \mu_{\text{FAC}}$. Our findings suggest that inclusive η_c production in Υ decay will provide a particularly clean laboratory to investigate the CO mechanism in charmonium production and so to shed light on the J/ψ polarization puzzle at hadron colliders, and we propose to carry out such measurements in the future.

APPENDIX: SDCS $\hat{\Gamma}_{mn}$ AT $\mathcal{O}(\alpha_s^3)$

Here we list our analytic results for the SDCs $\hat{\Gamma}_{mn}$ of the decay processes $\Upsilon \to H + X$ with $H = J/\psi, \eta_c, \chi_{cJ}, h_c$ at $\mathcal{O}(\alpha_s^3)$. We have

$$\hat{\Gamma}(b\bar{b}(^1S_0^{[8]}) \to c\bar{c}(^3S_1^{[8]}) + g) = \frac{5\pi^2 \alpha_s^3 (m_b^2 - m_c^2)}{72 m_b^4 m_c^3},$$

$$\hat{\Gamma}(b\bar{b}(^3S_1^{[8]}) \to c\bar{c}(^1S_0^{[1]}) + g) = \frac{\pi^2 \alpha_s^3 (m_b^2 - m_c^2)}{27 m_b^6 m_c},$$

$$\hat{\Gamma}(b\bar{b}(^3S_1^{[8]}) \to c\bar{c}(^1S_0^{[8]}) + g) = \frac{5\pi^2 \alpha_s^3 (m_b^2 - m_c^2)}{72 m_b^6 m_c},$$

$$\hat{\Gamma}(b\bar{b}(^3S_1^{[8]}) \to c\bar{c}(^1P_1^{[8]}) + g) = \frac{\pi^2\alpha_s^3(m_b^2 - m_c^2)}{24m_b^6 m_c^3},$$

$$\hat{\Gamma}(b\bar{b}(^3S_1^{[8]}) \to c\bar{c}(^3P_0^{[1]}) + g) = \frac{\pi^2\alpha_s^3(m_b^2 - 3m_c^2)^2}{81m_b^6 m_c^3(m_b^2 - m_c^2)},$$

$$\hat{\Gamma}(b\bar{b}(^3S_1^{[8]}) \to c\bar{c}(^3P_1^{[1]}) + g) = \frac{2\pi^2\alpha_s^3(m_b^2 + m_c^2)}{81m_b^4 m_c^3(m_b^2 - m_c^2)},$$

$$\hat{\Gamma}(b\bar{b}(^3S_1^{[8]}) \to c\bar{c}(^3P_2^{[1]}) + g) = \frac{2\pi^2\alpha_s^3(m_b^4 + 3m_b^2 m_c^2 + 6m_c^4)}{405m_b^6 m_c^3(m_b^2 - m_c^2)},$$

$$\sum_{J=0}^{2} \hat{\Gamma}(b\bar{b}(^3S_1^{[8]}) \to c\bar{c}(^3P_J^{[8]}) + g) = \frac{5\pi^2\alpha_s^3(3m_b^4 + 2m_b^2 m_c^2 + 7m_c^4)}{72m_b^6 m_c^3(m_b^2 - m_c^2)},$$

$$\sum_{J=0}^{2} \hat{\Gamma}(b\bar{b}(^3P_J^{[8]}) \to c\bar{c}(^3S_1^{[8]}) + g) = \frac{5\pi^2\alpha_s^3(7m_b^4 + 2m_b^2 m_c^2 + 3m_c^4)}{72m_b^6 m_c^3(m_b^2 - m_c^2)}. \tag{A1}$$

We note that, incidentally, $\hat{\Gamma}(b\bar{b}(^3S_1^{[8]}) \to c\bar{c}(^3S_1^{[8]}) + g) = 0$ at $\mathcal{O}(\alpha_s^3)$. Adopting the J/ψ LDMEs from Refs. [12,49] and the χ_{cJ} ones from Ref. [23] and deriving from them the η_c and h_c ones via the HQSS relations in Eq. (9), we find that the results for the ratios $\langle\Upsilon|\mathcal{O}(^1S_0^{[8]})|\Upsilon\rangle/\langle\Upsilon|\mathcal{O}(^3S_1^{[1]})|\Upsilon\rangle$ and $\langle\Upsilon|\mathcal{O}(^3S_8^{[8]})|\Upsilon\rangle/\langle\Upsilon|\mathcal{O}(^3S_1^{[1]})|\Upsilon\rangle$ determined in Ref. [34], namely $2.414(3) \times 10^{-3}$ and $8.1(6) \times 10^{-5}$ in the hybrid scheme and $9.0(1) \times 10^{-5}$ and $6.9(5) \times 10^{-5}$ in the nrqcd scheme, yield the $\mathcal{O}(\alpha_s^3)$ contributions to $\mathcal{B}_{\text{direct}}(\Upsilon \to H + X)$ specified in Table V. These results are μ independent thanks to the normalization in Eq. (6), which, for consistency, is evaluated here at LO. They still need to be supplemented by the contributions proportional to $\langle\Upsilon|\mathcal{O}(^3P_0^{[8]})|\Upsilon\rangle$, which is still unknown.

---

[1] W. E. Caswell and G. P. Lepage, Effective lagrangians for bound state problems in QED, QCD, and other field theories, Phys. Lett. **167B**, 437 (1986).

[2] G. T. Bodwin, E. Braaten, and G. P. Lepage, Rigorous QCD analysis of inclusive annihilation and production of heavy quarkonium, Phys. Rev. D **51**, 1125 (1995); Erratum, Phys. Rev. D **55**, 5853 (1997).

[3] G. P. Lepage, L. Magnea, C. Nakhleh, U. Magnea, and K. Hornbostel, Improved nonrelativistic QCD for heavy-quark physics, Phys. Rev. D **46**, 4052 (1992).

[4] N. Brambilla *et al.*, Heavy quarkonium: progress, puzzles, and opportunities, Eur. Phys. J. C **71**, 1534 (2011).

[5] N. Brambilla *et al.*, QCD and strongly coupled gauge theories: challenges and perspectives, Eur. Phys. J. C **74**, 2981 (2014).

[6] J.-P. Lansberg, New Observables in Inclusive Production of Quarkonia, arXiv:1903.09185.

[7] Y.-J. Zhang, Y.-Q. Ma, K. Wang, and K.-T. Chao, QCD radiative correction to color-octet J/ψ inclusive production at B factories, Phys. Rev. D **81**, 034015 (2010).

[8] Y.-Q. Ma, Y.-J. Zhang, and K.-T. Chao, QCD Corrections to $e^+e^- \to J/\psi + gg$ at B Factories, Phys. Rev. Lett. **102**, 162002 (2009).

[9] B. Gong and J.-X. Wang, Next-to-Leading-Order QCD Corrections to $e^+e^- \to J/\psi gg$ at the B Factories, Phys. Rev. Lett. **102**, 162003 (2009).

[10] M. Klasen, B. A. Kniehl, L. N. Mihaila, and M. Steinhauser, J/ψ plus jet associated production in two-photon collisions at next-to-leading order, Nucl. Phys. **B713**, 487 (2005).

[11] M. Klasen, B. A. Kniehl, L. N. Mihaila, and M. Steinhauser, J/ψ plus prompt-photon associated production in two-photon collisions at next-to-leading order, Phys. Rev. D **71**, 014016 (2005).

[12] M. Butenschoen and B. A. Kniehl, World data of J/ψ production consolidate nonrelativistic QCD factorization at next-to-leading order, Phys. Rev. D **84**, 051501(R) (2011).

[13] M. Butenschön and B. A. Kniehl, Complete Next-to-Leading-Order Corrections to J/ψ Photoproduction in Nonrelativistic Quantum Chromodynamics, Phys. Rev. Lett. **104**, 072001 (2010).

[14] M. Butenschön and B. A. Kniehl, Probing Nonrelativistic QCD Factorization in Polarized J/ψ Photoproduction at Next-to-Leading Order, Phys. Rev. Lett. **107**, 232001 (2011).

[15] Y.-Q. Ma, K. Wang, and K.-T. Chao, $J/\psi(\psi')$ Production at the Tevatron and LHC at $\mathcal{O}(\alpha_s^4 v^4)$ in Nonrelativistic QCD, Phys. Rev. Lett. **106**, 042002 (2011).

[16] M. Butenschön and B. A. Kniehl, Reconciling J/ψ Production at HERA, RHIC, Tevatron, and LHC with Nonrelativistic QCD Factorization at Next-to-Leading Order, Phys. Rev. Lett. **106**, 022003 (2011).

[17] M. Butenschoen and B. A. Kniehl, J/ψ Polarization at the Tevatron and the LHC: Nonrelativistic-QCD Factorization at the Crossroads, Phys. Rev. Lett. **108**, 172002 (2012).

[18] K.-T. Chao, Y.-Q. Ma, H.-S. Shao, K. Wang, and Y.-J. Zhang, J/ψ Polarization at Hadron Colliders in Nonrelativistic QCD, Phys. Rev. Lett. **108**, 242004 (2012).

[19] B. Gong, L.-P. Wan, J.-X. Wang, and H.-F. Zhang, Polarization for Prompt J/ψ and $\psi(2s)$ Production at the Tevatron and LHC, Phys. Rev. Lett. **110**, 042002 (2013).

[20] H.-S. Shao, H. Han, Y.-Q. Ma, C. Meng, Y.-J. Zhang, and K.-T. Chao, Yields and polarizations of prompt J/ψ and $\psi(2S)$ production in hadronic collisions, J. High Energy Phys. 05 (2015) 103.

[21] M. Butenschoen, Z.-G. He, and B. A. Kniehl, η_c Production at the LHC Challenges Nonrelativistic QCD Factorization, Phys. Rev. Lett. **114**, 092004 (2015).

[22] R. Aaij et al. (LHCb Collaboration), Measurement of the $\eta_c(1S)$ production cross-section in proton-proton collisions via the decay $\eta_c(1S) \to p\bar{p}$, Eur. Phys. J. C **75**, 311 (2015).

[23] Z.-G. He, B. A. Kniehl, and X.-P. Wang, Inclusive χ_{cJ} production in Υ decay at $\mathcal{O}(\alpha_s^5)$ in NRQCD factorization, Phys. Rev. D **98**, 074005 (2018).

[24] R. Fulton et al. (CLEO Collaboration), First observation of inclusive ψ production in Υ decays, Phys. Lett. B **224**, 445 (1989).

[25] W. Maschmann et al. (Crystal Ball Collaboration), Inclusive J/ψ production in decays of B mesons, Z. Phys. C **46**, 555 (1990).

[26] H. Albrecht et al. (ARGUS Collaboration), Search for charm production in direct decays of the $\Upsilon(1S)$ resonance, Z. Phys. C **55**, 25 (1992).

[27] R. A. Briere et al. (CLEO Collaboration), New measurements of $\Upsilon(1S)$ decays to charmonium final states, Phys. Rev. D **70**, 072001 (2004).

[28] C. P. Shen et al. (Belle Collaboration), Search for XYZ states in $\Upsilon(1S)$ inclusive decays, Phys. Rev. D **93**, 112013 (2016).

[29] M. Tanabashi et al. (Particle Data Group), Review of Particle Physics, Phys. Rev. D **98**, 030001 (2018).

[30] K. Cheung, W.-Y. Keung, and T. C. Yuan, Color-octet J/ψ production in the Υ decay, Phys. Rev. D **54**, 929 (1996).

[31] M. Napsuciale, Inclusive J/ψ production in Υ decay via color octet mechanisms, Phys. Rev. D **57**, 5711 (1998).

[32] Z.-G. He and J.-X. Wang, Inclusive J/ψ production in Υ decay via color-singlet mechanism, Phys. Rev. D **81**, 054030 (2010).

[33] Z.-G. He and J.-X. Wang, Color-singlet J/ψ production at $\mathcal{O}(\alpha_s^6)$ in Υ decay, Phys. Rev. D **82**, 094033 (2010).

[34] G. T. Bodwin, J. Lee, and D. K. Sinclair, Spin correlations and velocity scaling in color-octet nonrelativistic QCD matrix elements, Phys. Rev. D **72**, 014009 (2005).

[35] T. Hahn, Generating Feynman diagrams and amplitudes with FeynArts 3, Comput. Phys. Commun. **140**, 418 (2001).

[36] R. Mertig, M. Böhm, and A. Denner, Feyn Calc—Computer-algebraic calculation of Feynman amplitudes, Comput. Phys. Commun. **64**, 345 (1991).

[37] J. Kuipers, T. Ueda, J. A. M. Vermaseren, and J. Vollinga, FORM version 4.0, Comput. Phys. Commun. **184**, 1453 (2013).

[38] F. Feng, $Apart: A generalized MATHEMATICA Apart function, Comput. Phys. Commun. **183**, 2158 (2012).

[39] A. V. Smirnov, Algorithm FIRE—Feynman Integral REduction, J. High Energy Phys. 10 (2008) 107.

[40] S. Carrazza, R. K. Ellis, and G. Zanderighi, QCDLoop: A comprehensive framework for one-loop scalar integrals, Comput. Phys. Commun. **209**, 134 (2016).

[41] T. Hahn, CUBA—a library for multidimensional numerical integration, Comput. Phys. Commun. **168**, 78 (2005).

[42] J. G. Körner, J. H. Kühn, M. Krammer, and H. Schneider, Zweig-forbidden radiative orthoquarkonium decays in perturbative QCD, Nucl. Phys. **B229**, 115 (1983).

[43] B. W. Harris and J. F. Owens, Two cutoff phase space slicing method, Phys. Rev. D **65**, 094032 (2002).

[44] M. Butenschön, Photoproduction of the J/ψ meson at HERA at next-to-leading order within the framework of nonrelativistic QCD, Report No. DESY-THESIS-2009-021.

[45] S.-y. Li, Q.-b. Xie, and Q. Wang, Contribution of colour-singlet process $\Upsilon \to J/\psi + c\bar{c}g$ to $\Upsilon \to J/\psi + X$, Phys. Lett. B **482**, 65 (2000).

[46] G. Grunberg, Renormalization group improved perturbative QCD, Phys. Lett. **95B**, 70 (1980); Erratum, Phys. Lett. **110B**, 501(E) (1982).

[47] P. B. Mackenzie and G. P. Lepage, Quantum Chromodynamic Corrections to the Gluonic Width of the Υ Meson, Phys. Rev. Lett. **47**, 1244 (1981).

[48] H. Han, Y.-Q. Ma, C. Meng, H.-S. Shao, and K.-T. Chao, η_c Production at LHC and Implications for the Understanding of J/ψ Production, Phys. Rev. Lett. **114**, 092005 (2015).

[49] M. Butenschoen and B. A. Kniehl, J/ψ production in NRQCD: A global analysis of yield and polarization, Nucl. Phys. B, Proc. Suppl. **222**–**224**, 151 (2012).

[50] G. T. Bodwin, K.-T. Chao, H. S. Chung, U-R. Kim, J. Lee, and Y.-Q. Ma, Fragmentation contributions to hadroproduction of prompt J/ψ, χ_{cJ}, and $\psi(2S)$ states, Phys. Rev. D **93**, 034041 (2016).

[51] E. J. Eichten and C. Quigg, Quarkonium wave functions at the origin, Phys. Rev. D **52**, 1726 (1995).

[52] W. Buchmüller and S.-H. H. Tye, Quarkonia and quantum chromodynamics, Phys. Rev. D **24**, 132 (1981).